Properties of Elliptical Galaxies

The first step in investigating the evolution of galaxies is to understand the properties of those galaxies today. We'll start with the elliptical galaxies, which are basically very old stellar populations, with little evidence of recent star formation. We can summarize their properties as follows:

• In general, elliptical galaxies, as projected on the sky, have complete 2-dimensional symmetry. The question of whether these objects are symmetric in practice, or are tri-axial is open (though dynamical modeling suggests that triaxiality can only last for a short time). Some ellipticals have "fine structure," such as very weak ripples, shells, and boxy (not elliptical) isophotes. These signatures are weak, but real. In general, those ellipticals with fine structure are *slightly* bluer than equivalent galaxies without fine structure. Disky ellipticals also have more rotation than boxy ellipticals; the latter have very low values of v/σ.

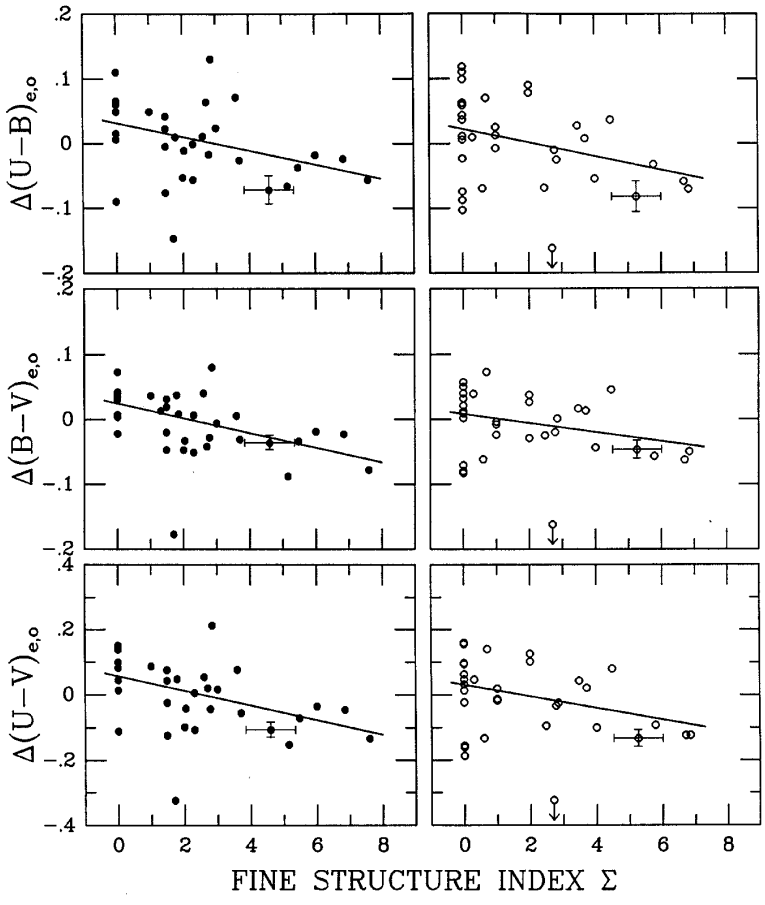

FIG. 2. Correlations between color residuals and fine-structure index Σ for 35 ellipticals (left, solid dots) and 34 S0 galaxies (right, open circles). The residuals for ellipticals were determined from least-squares fits to 227 E galaxies (see Table 2), and those for S0 galaxies from fits to 241 S0's. Solid lines mark the mean ΔC_r–Σ relations given in Table 3. Note that the color residuals, and by implication the colors themselves, get systematically bluer as Σ increases.

[Schweizer & Seitzer 1992, *A.J.* **104,** 1039]

• Ellipticals range in flattening from E0 (round) to E7. No elliptical is flatter than E7. The data are *not* consistent with the hypothesis that all ellipticals are E7 and appear rounder by the effects of random viewing angles. Most likely there is a spread of flattenings centered around E3, or thereabouts. Their flattening is also inconsistent with the idea of rotational support – rotation is unimportant in most systems.

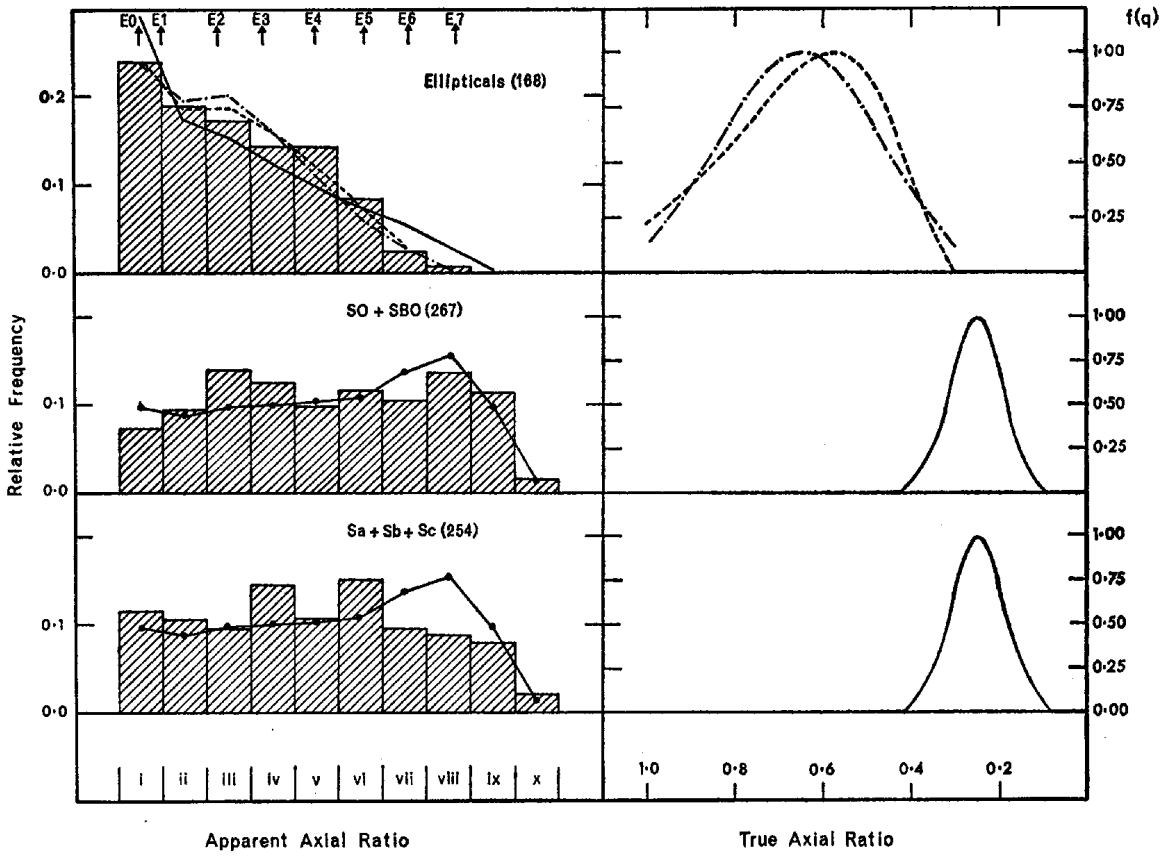

FIG. 1.—*Left*, histograms of the distribution of apparent axial ratios for E, S0, and spiral galaxies, sorted into class intervals defined in Tables 1 and 2. The curves are predicted ratios for various assumptions of the distribution of intrinsic flattening. *Right*, assumed intrinsic distributions corresponding to the curves on the left. The case of uniform flattening for E galaxies is a straight horizontal line truncated at $b/a = 0.3$ and is not shown. Dot-dash curve is a Gaussian with $q_0 = 0.65$ and $\sigma = 0.18$. Dashed curve is a skewed binomial distribution defined in the text, with $q_0 = 0.58$, $a = 0.31$, and $p = 3.0$. The two solid curves are Gaussians with $q_0 = 0.25$ and $\sigma = 0.06$.

[Sandage, Freeman, & Stokes 1970, *Ap.J.*, **160,** 831]

• There is little or no star formation in elliptical galaxies. However, the spectral energy distribution of some ellipticals turns up in the ultraviolet. (In other words, since elliptical galaxies are made up of old stars, the composite spectrum of an elliptical should look like that of a $\sim 4,000°$ K star. However, many ellipticals are brighter at 1500 Å than they are at 2000 Å.)

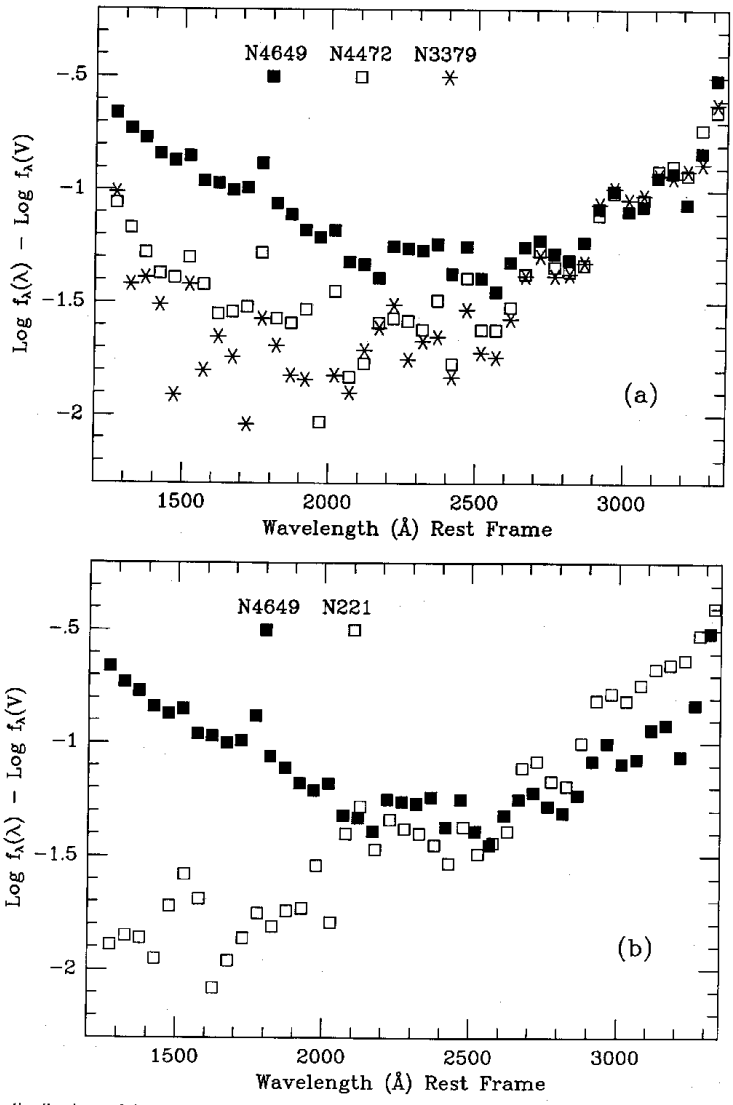

FIG. 4.—(*a*) Ultraviolet energy distributions of three quiescent galaxies that span the maximum range in Mg_2. All three galaxies have similar energy distributions from 2600 to 3200 Å, despite a relatively wide intrinsic range in the strengths of optical absorption-line features. This demonstrates that the blue light contamination in these galaxies is significant even at 3000 Å (see also Fig. 8). (*b*) The quiescent galaxy with the strongest optical absorption lines, N4649, vs. the galaxy with the weakest lines, NGC 221. The cross-over of the ultraviolet spectra further demonstrates the measurable amount of blue light contamination near 2600 Å in NGC 4649.

[Burstein *et al.* 1988, *Ap.J.*, **328**, 440]

• There is very little cold interstellar medium in elliptical galaxies. However, there is x-ray gas at a temperature of about $T \sim 10^6$ K. One can easily see where this gas comes from. The stars in an elliptical galaxy must be losing mass. If the stars are moving isotropically at $\sigma \sim 200$ km s^{-1}, then the atoms of lost material, if thermalized, will have a temperature of

$$\frac{1}{2} m_H \sigma^2 \sim \frac{3}{2} kT \Longrightarrow \ T \sim 10^6 \text{ degrees K} \qquad (6.01)$$

• Most ellipticals have weak radial color gradients: they are redder on the inside than they are on the outside. This may be due to age (older stars have a redder turn-off mass), or metallicity (metal-rich stars are intrinsically redder than their metal-poor counterparts, due to the effects of H^- opacity and the line-blanketing of metals).

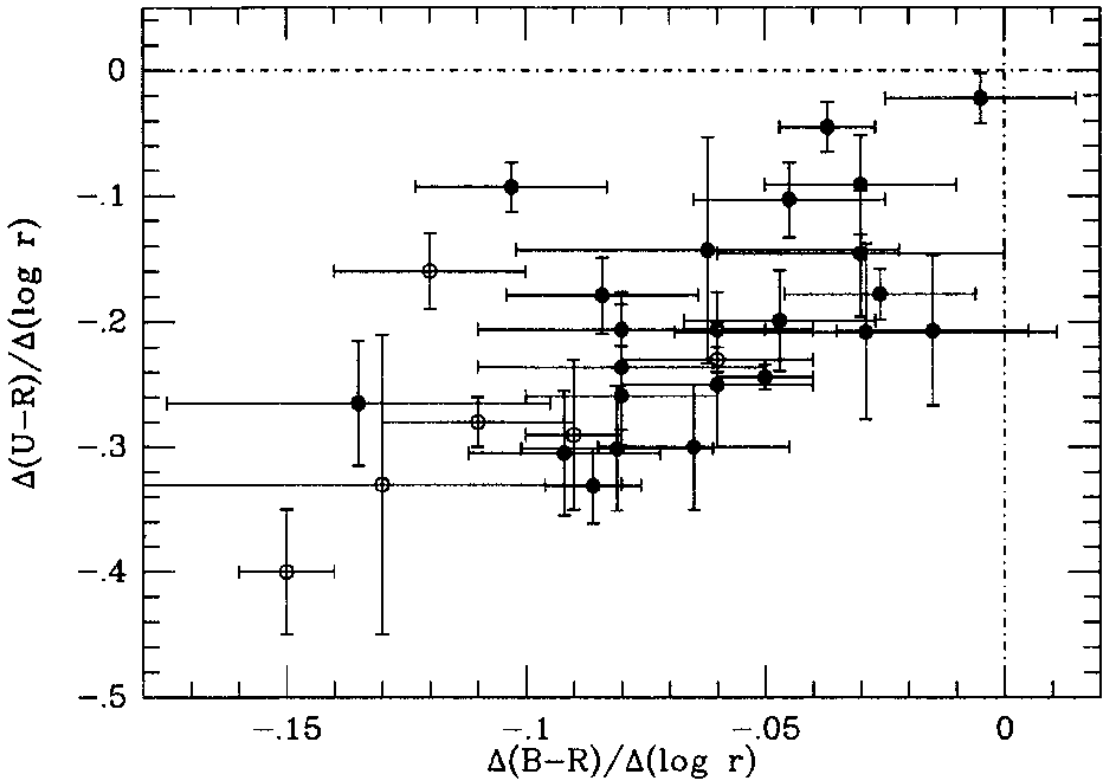

FIG. 11. Logarithmic color gradients in $U - R$ in mag dex^{-1} against color gradients in $B - R$. There is a correlation, but it is weaker than might be expected. This is mainly due to the large scatter in $\Delta(B - R)$ from observational uncertainty.

[Peletier *et al.* 1990, *A.J.*, **100,** 1091]

• There appears to be a correlation between the mass of an elliptical galaxy (or the bulge of a spiral galaxy) and its central black hole.

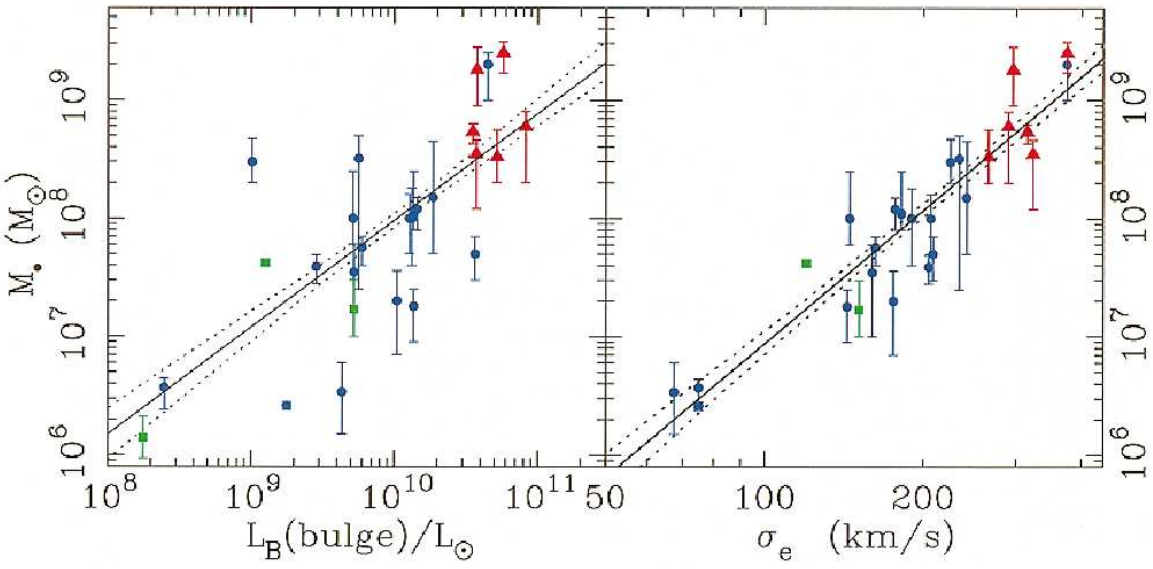

FIG. 2.—Black hole mass versus bulge luminosity (*left*) and the luminosity-weighted aperture dispersion within the effective radius (*right*). There are 26 points in the dispersion plot; 13 are new detections from stellar kinematics (K. Gebhardt et al. 2000, in preparation; G. Bower et al. 2000, in preparation). Green squares denote galaxies with maser detections, red triangles are from gas kinematics, and blue circles are from stellar kinematics. Solid and dotted lines are the best-fit correlations and their 68% confidence bands.

[Ferrarese & Merritt 2000, *Ap.J. (Letters)*, **539,** L9]
[Gebhardt, *et al.* 2000, *Ap.J. (Letters)*, **539,** L13]

The Elliptical Galaxy Fundamental Plane

Elliptical galaxies populate a "fundamental plane" in luminosity-surface brightness-velocity dispersion space. At first glance, the physics underlying this plane is easy to understand.

If you assume the stars of an elliptical galaxy are in virial equilibrium, then their typical velocity dispersion will be

$$\sigma^2 \propto \frac{\mathcal{M}}{R} \tag{6.02}$$

Now let's assume that all elliptical galaxies have the same mass-to-light ratio ($\mathcal{L} \propto \mathcal{M}$) and all have about the same surface brightness ($I = \mathcal{L}/R^2$). Then, if I is indeed a constant,

$$\sigma^2 \propto \frac{\mathcal{M}}{R} \propto \frac{\mathcal{L}}{R} \propto \frac{\mathcal{L}}{\mathcal{L}^{1/2}} \propto \mathcal{L}^{1/2} \Longrightarrow \mathcal{L} \propto \sigma^4 \tag{6.03}$$

This is called the *Faber-Jackson relation*. The velocity dispersion, σ is usually measured near the galactic nucleus, where the galaxy is brightest (and a high signal-to-noise spectrum is obtainable).

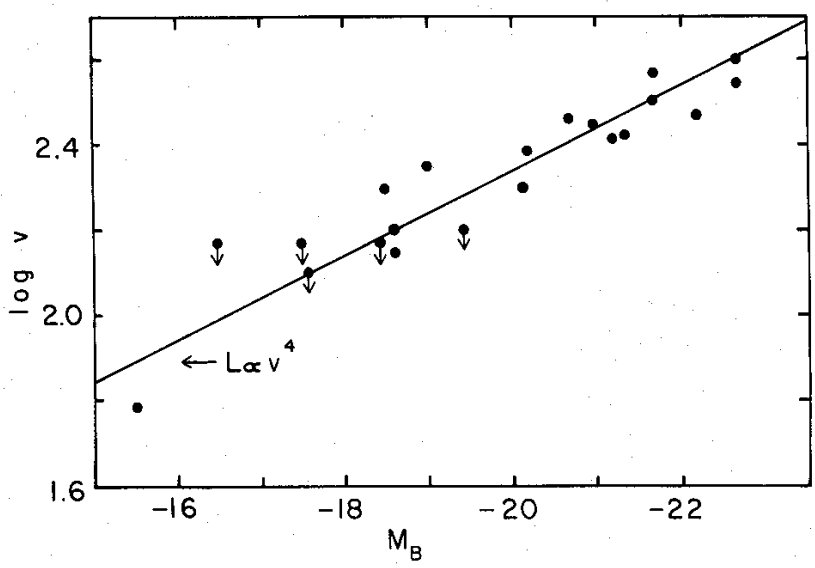

FIG. 16.—Line-of-sight velocity dispersions versus absolute magnitude from Table 1. The point with smallest velocity corresponds to M32, for which the velocity dispersion (60 km s^{-1}) was taken from Richstone and Sargent (1972).

[Faber & Jackson, *Ap.J.*, **204,** 668]

Of course, all galaxies do not have the same surface brightness. So if you take $I = \mathcal{L}/R^2$ and substitute that into the virial theorum (keeping the mass-to-light ratio assumption), then a relation between luminosity, surface brightness, and velocity dispersion is the natural consequence, *i.e.,*

$$\mathcal{L} \propto \sigma^4 I^{-1} \tag{6.04}$$

Observations of real ellipticals show that when $\mathcal{L}$ is the total B-band luminosity of the galaxy, σ is the central velocity dispersion, and I is the galaxy surface brightness measured at a radius that contains 1/2 the total light from the galaxy (R_e), the coefficients in (11.03) are not 4 and -1, but 2.7 and -0.7. This is the elliptical galaxy fundamental plane.

Note that (4.04) can be simplified. Dimensionally speaking, luminosity divided by surface brightness ($\mathcal{L}/I$) has the units of size squared. Thus, one group (who called themselves the Seven Samurai) combined the two variables, and took the square root, thereby creating a new characteristic size variable, D_n. (Their specific definition for D_n was that of a circular aperture that enclosed a mean blue surface brightness of 20.75 mag arcsec^{-2}, but other definitions are possible.) The best fit to the authors' (very large) dataset yielded

$$D_n \propto \sigma^{1.2} \tag{6.05}$$

Thus, the $D_n - \sigma$ relation is actually just the optimal projection of the fundamental plane into a single dimension.

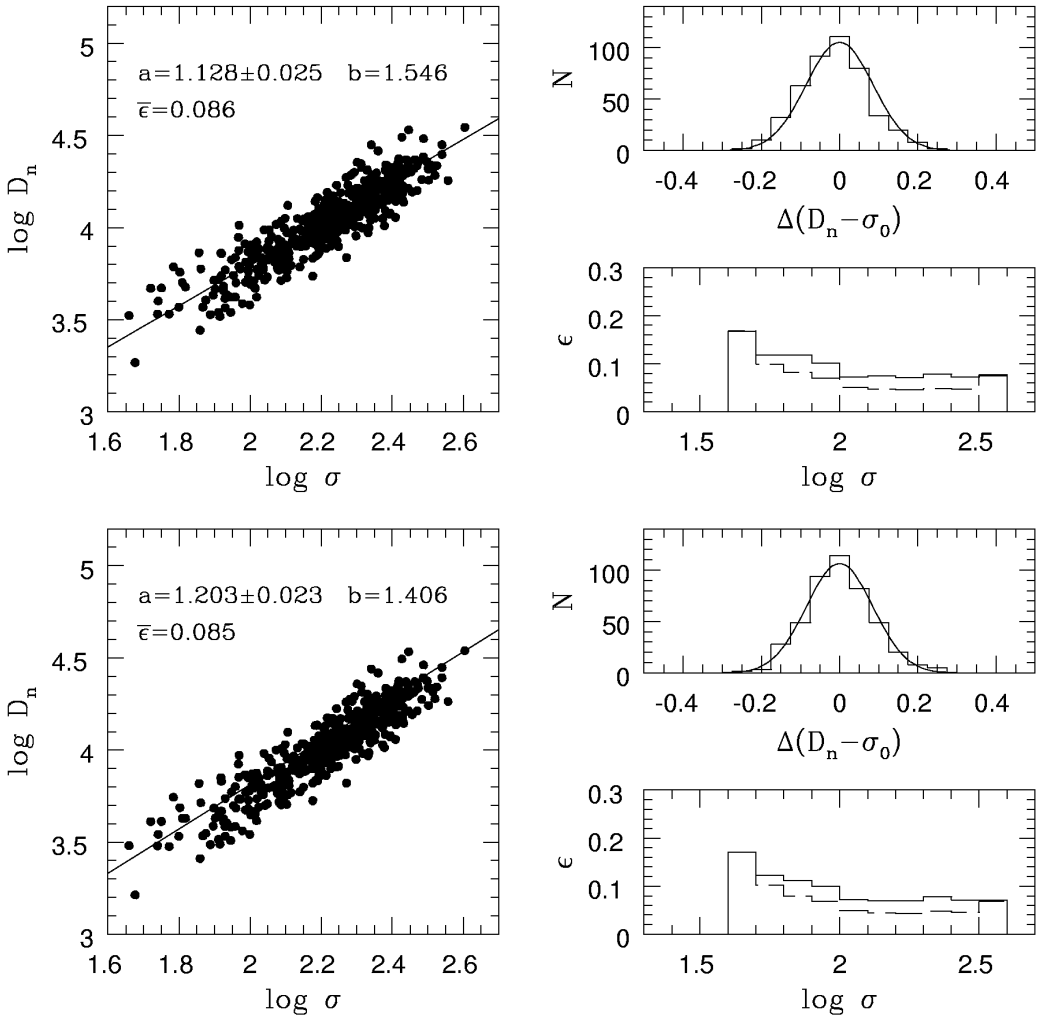

FIG. 4.—*Left panels:* Measurements before the bias correction is applied (*upper panel*) and the final corrected values derived from the iterative process (*lower panel*) as a function of σ. The line shows the derived distance relation. The values of the slope (a), zero point (b), and mean rms scatter ($\overline{\epsilon}$) are also shown. *Right panels:* Distribution of the residuals relative to the D_n-σ relation, as well as the distribution of the corresponding observed scatter (*solid line*) and intrinsic scatter (*dashed line*) as a function of σ.

[Dressler *et al.* 1987, *Ap. J.*, **313,** 42]
[Bernardi *et al.* 2002, *A.J.*, **123,** 2159]

The elliptical galaxy fundamental plane is one of the least accurate of the reliable extragalactic standard candles – it's scatter can be up to $\sim 20\%$. In part, this may be caused by its reliance on the galaxy's central velocity dispersion, which may be affected by local conditions. However, since elliptical galaxies are found in clusters, one usually improves the distance estimates by analyzing multiple galaxies, and beating the dispersion down by by $\sqrt{N}$.

Interestingly, the fundamental plane is not just a relation between luminosity, size, and velocity dispersion. The relationship is reflected in many other variables. For example,

• Elliptical galaxy luminosity correlates with color. Large ellipticals are redder than small ellipticals.

• Elliptical galaxy luminosities (or velocity dispersions) correlate with absorption line strength. Bright, redder galaxies have stronger absorption features.

• Elliptical galaxy absorption features correlate with the UV upturn. Galaxies with strong absorption features have larger UV excesses.

• Elliptical galaxy UV excess correlates with the number of planetary nebulae in the galaxy. Galaxies with large UV excesses have, relatively speaking, fewer planetary nebulae.

Any of the above variables can be substituted in for the others to form a tight correlation of properties. The existence of the fundamental plane argues strongly that elliptical galaxies, as a class, are very homogeneous in their properties.

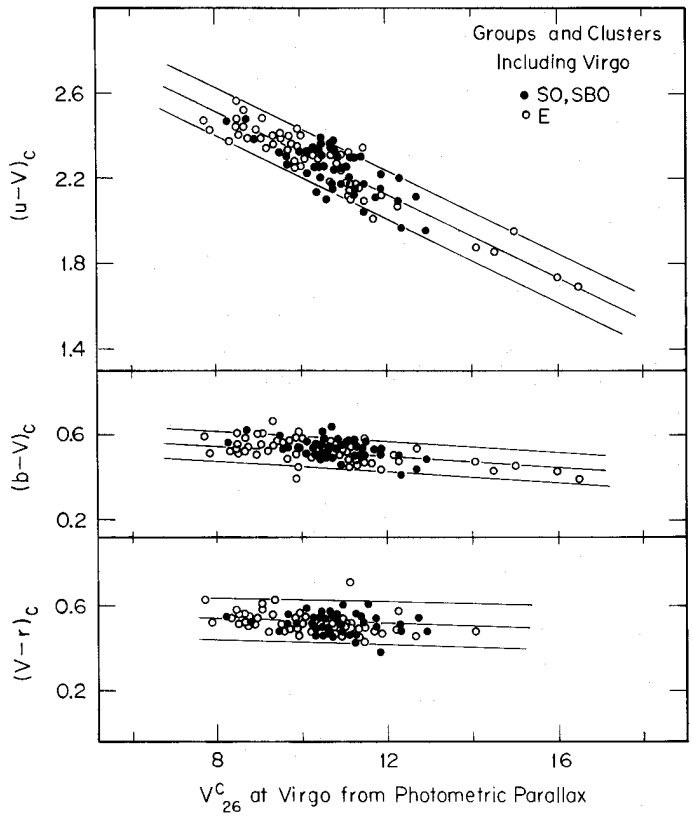

FIG. 7.—Composite C-M diagram for all galaxies in the sample, shifted to the Virgo cluster distance by magnitude differences calculated from the photometric parallaxes. Galaxies of E and S0 types are shown with different symbols. The ridge line is the Virgo cluster solution of Fig. 3. Boundary lines are at $\pm 2\,\sigma$ in the color residuals.

[Visvanathan & Sandage 1977, *Ap.J.*, **216**, 214]

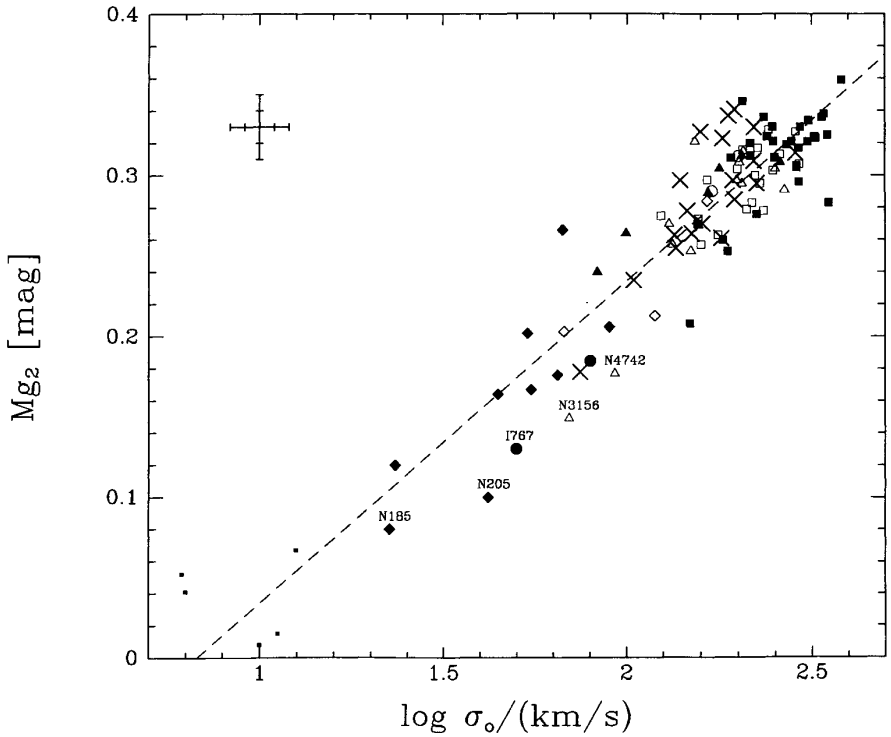

FIG. 3.—Nuclear Mg_2 index plotted against σ_0 for all types of DHGs (symbols coded as in Fig. 1). The dotted line represents the relation $Mg_2 = 0.20 \log \sigma_0 - 0.166$. Galaxies which show evidence for young or intermediate age stars are labeled. Representative error bars are shown in the upper left, the larger error bars refer to the objects with low values of σ_0, the smaller ones to luminous ellipticals and bulges. The Mg_2–log σ_0 correlation is tight over many decades in galaxy size and all DHG types.

[Bender, Burstein, & Faber 1993, *Ap.J.*, **411**, 153]

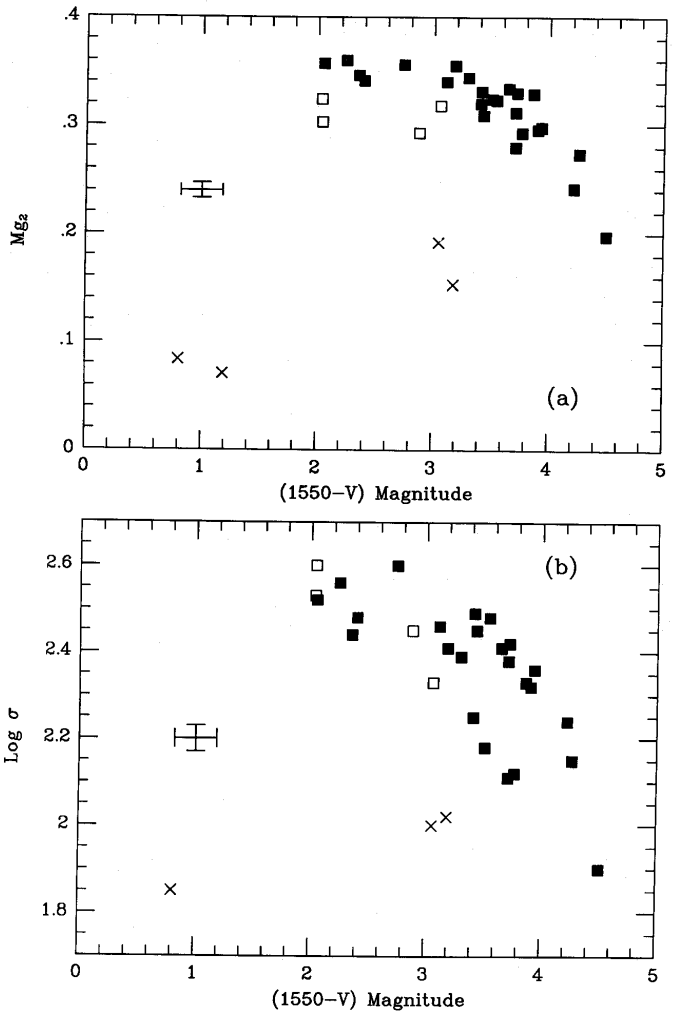

FIG. 1.—(*a*) The optical absorption-line index Mg_2 plotted vs. the ultraviolet/optical (1550 − *V*) color (expressed in magnitudes) for the 32 galaxies in this sample. Closed squares represent "quiescent" galaxies, open squares represent "active" galaxies, and crosses represent galaxies with on-going star formation. (*b*) Central velocity dispersions for 31 of the galaxies (NGC 205 excepted) vs. (1550 − *V*) color. Along with larger intrinsic scatter, there is no separation of active and quiescent galaxies in this plot.

[Burstein *et al.* 1988, *Ap.J.*, **328**, 440]

Elliptical Galaxy Surface Brightness Profiles

There are several ways to approximate the observed luminosity profile of elliptical galaxies. Let R be the projected radius of the galaxy, r the true space, radius, $I(R)$ the observed surface brightness, and $j(r)$ the actual luminosity as a function of true space radius. (Remember, the light you see at a distance R is the sum of the line-of-sight through the galaxy.)

[Reynolds 1913, *MNRAS,* **74,** 132]
[Hubble 1930, *Ap.J.,* **71,** 231]

The original description of an elliptical galaxy's surface brightness was

$$I(R) = \frac{I_0}{(R/a+1)^2} \tag{6.06}$$

or, in terms of magnitudes

$$m(R) = m_0 + 5\log\left(\frac{R}{a}+1\right) \tag{6.07}$$

where a is the galaxy's characteristic radius. This law had the advantage that it was simple and, at large radii, it resembled an isothermal sphere. However, it implies a non-analytic form for the true space density, j. Also, the total luminosity of the galaxy is

$$\begin{aligned}
\mathcal{L} &= \int_0^\infty 2\pi R \left\{ \frac{I_0}{((R/a)+1)^2} \right\} dR \\
&= 2\pi a^2 I_0 \int_0^\infty \frac{R}{(R+a)^2} dR \\
&\quad 2\pi a^2 I_0 \left\{ \ln(R+a) + \frac{a}{(R+a)} \right\} \Bigg|_0^\infty \\
&= \infty
\end{aligned} \tag{6.08}$$

THE DE VAUCOULEURS LAW

[de Vaucouleurs 1959, *Handbuch der Physik*]
[Young 1976, *A.J.*, **81,** 807]

The most famous description of an elliptical galaxy is the de Vaucouleur $R^{1/4}$-law. According to the law, the surface brightness, in terms of magnitudes

$$m_R = a + bR^{1/4} \tag{6.09}$$

Most times, a and b are not quoted: instead, one parameterizes the galaxy in terms of the effective radius, R_e, and the surface brightness (in magnitudes) at R_e. R_e is defined as the observed radius of the galaxy which encloses half the total light. To relate a and b to R_e and m_e, one starts with

$$m = a + bR^{1/4} \qquad m_e = a + bR_e^{1/4} \tag{6.10}$$

and differences these two equations

$$m - m_e = b\left\{R^{1/4} - R_e^{1/4}\right\} = bR_e^{1/4}\left\{(R/R_e)^{1/4} - 1\right\} \tag{6.11}$$

or

$$\log(I/I_e) = -\left(\frac{bR_e^{1/4}}{2.5}\right)\left\{(R/R_e)^{1/4} - 1\right\} \tag{6.12}$$

Since R_e by definition encloses half the light

$$\mathcal{L}(R_e) = \int_0^{R_e} 2\pi R \cdot I(R)dR = \int_0^{R_e} 2\pi R \cdot C \cdot 10^{-0.4(a+bR^{1/4})}dR \tag{6.13}$$

and

$$\begin{aligned}\frac{\mathcal{L}(R_e)}{\mathcal{L}_T} &= \int_0^{R_e} R \cdot e^{-0.4\ln(10)bR^{1/4}}dR \Bigg/ \int_0^{\infty} R \cdot e^{-0.4\ln(10)bR^{1/4}}dR \\ &= 0.5\end{aligned} \tag{6.14}$$

where C is the zero-point constant for the magnitude system. A (numerical) solution to this equation yields $bR_e^{1/4} = 8.327$. If one then substitutes this back in (4.12), one then gets the alternative form of the de Vaucouleurs law

$$\log\left(\frac{I}{I_e}\right) = -3.33071\left\{\left(\frac{R}{R_e}\right)^{1/4} - 1\right\} \tag{6.15}$$

where a and b are related to R_e and m_e via

$$R_e = \left(\frac{8.327}{b}\right)^4 \qquad m_e = a + 8.327 \tag{6.16}$$

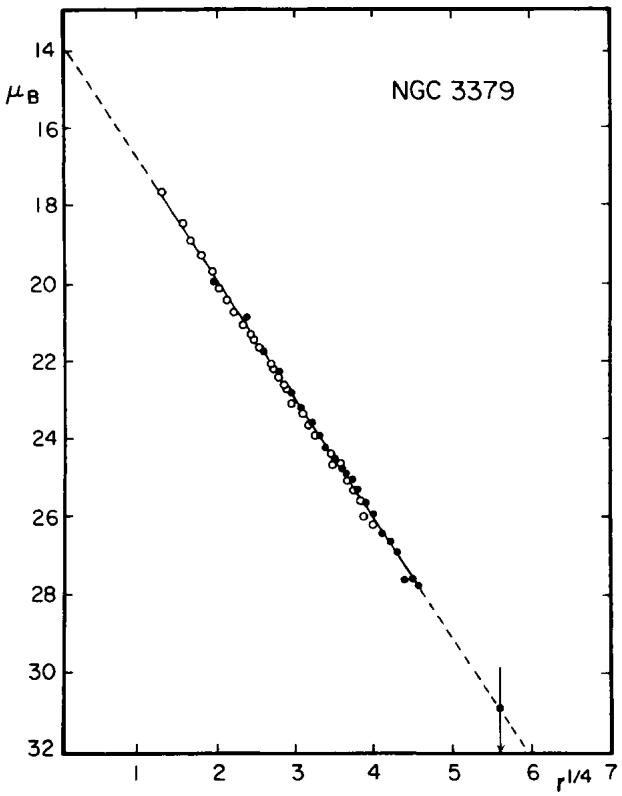

FIG. 2.—Mean E-W luminosity profile of NGC 3379 derived from McDonald photoelectric data. ●, Pe 4 data with 90 cm reflector; ○, Pe 1 data (M + P) with 2 m reflector. Note close agreement with $r^{1/4}$ law.

The advantages of the de Vaucouleurs law is that it is simple (in terms of magnitudes) and delivers total galactic luminosity that is finite and reasonable. Specifically, the expression for total luminosity

$$\mathcal{L}_T = \int_0^\infty 2\pi R \cdot 10^{+0.4(C-a-bR^{1/4})} dR \tag{6.17}$$

has the form

$$\mathcal{L} \propto \int_0^\infty x^7 e^{-ax} dx \tag{6.18}$$

and has the analytic solution

$$\mathcal{L}_T = 10^{-0.4(C-a)} \cdot \frac{\pi 8!}{(0.4 \ln(10) b)^8} \tag{6.19}$$

or

$$m_T = m_e - 3.388 - 5 \log R_e \tag{6.20}$$

The proof, which involves integrating by parts 7 times, is left to the ambitious student.

The disadvantages of the de Vaucouleurs law is that the space density (and galactic potential) implied by the law is non-analytic, so it is not convenient for modeling efforts.

THE JAFFE AND HERNQUIST LAWS

[Jaffe 1983, *MNRAS,* **202,** 995]
[Hernquist 1990, *Ap.J.,* **356,** 359]

There are two other laws that are used to model the luminosity profile of elliptical galaxies, the Jaffe law

$$j(r) = \frac{\mathcal{L} r_J}{4\pi r^2 (r + r_J)^2} \tag{6.21}$$

and the Hernquist model

$$j(r) = \frac{\mathcal{L}}{2\pi} \frac{a}{r(r+a)^3} \tag{6.22}$$

Note the different variables. The Hubble and de Vaucouleurs laws were observationally defined, hence R is the projected radius of the galaxy (observed on the sky) and I the observed surface brightness. For the Jaffe and Hernquist models, r is a 3-dimensional radius, and j a luminosity density (energy per volume, instead of per area). In above equations, r_J and a are the free parameters that define the fit. For the Jaffe model, r_J is the space radius that contains half the light, and $R_e = 0.763 r_J$; for the Hernquist model, a is the radius that contains one-quarter of the light, with $R_e = 1.8153a$. Both these laws have many useful analytic relations; the following appendix describes their properties.

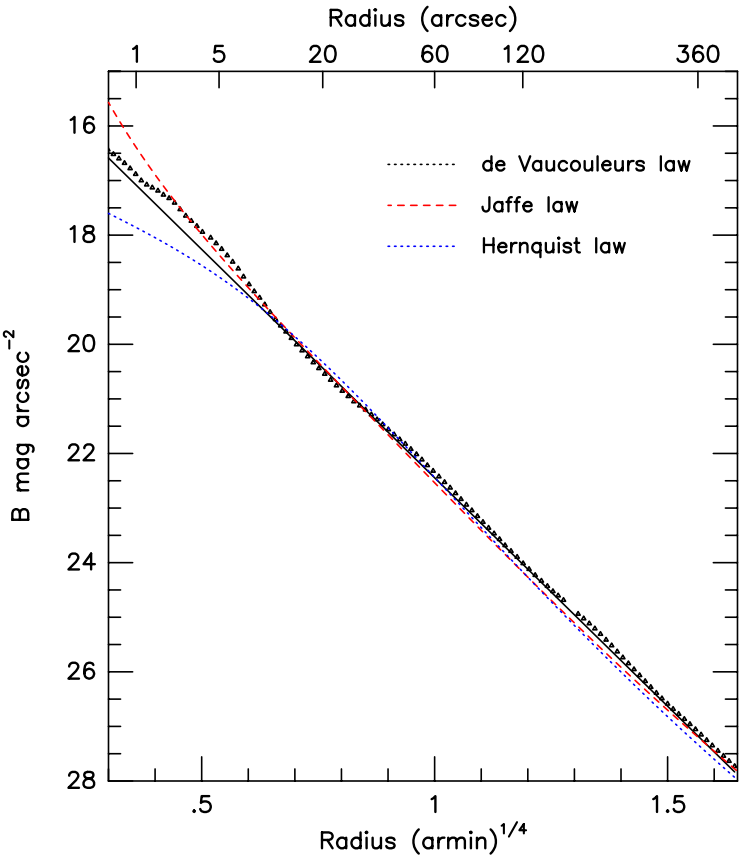

The de Vaucouleurs, Jaffe, and Hernquist surface brightness profiles of NGC 3379. The small triangles are the actual measurements of the galaxy.

Properties of Spiral Galaxies

The properties of spiral galaxies can be summarized as follows:

• Classically speaking, most spiral galaxies can be de-composed into an elliptical galaxy-like bulge, and an exponential law disk. In other words, in the absense of a bulge, the surface brightness of a spiral galaxy is simply

$$\left(\frac{I}{I_0}\right) = e^{-r/r_d} \tag{7.01}$$

where I_0 is the galaxy's central surface brightness in units of ergs-cm^{-2}-s^{-1}-arcsec^{-2} and r_d is the scale length of the exponential. However, not all spiral galaxies have a bulge, and in some galaxies (such as M31), a de-composition into a de-Vaucouleur bulge plus an exponential disk does not work very well. Another model of a spiral galaxy consists of an exponential "thin disk" plus a "thick disk" that may (or may not) be an extension of the thin disk, and may (or may not) be an extension of the bulge.

• Although the surface brightness of a disk declines exponentially, the e-folding scale length is generally not the scale length you measure in the optical. The amount of internal extinction also declines with radius, effectively flattening the brightness distribution of the disk. (The effect is greater in high-inclination galaxies, where the total amount of extinction is greatest.)

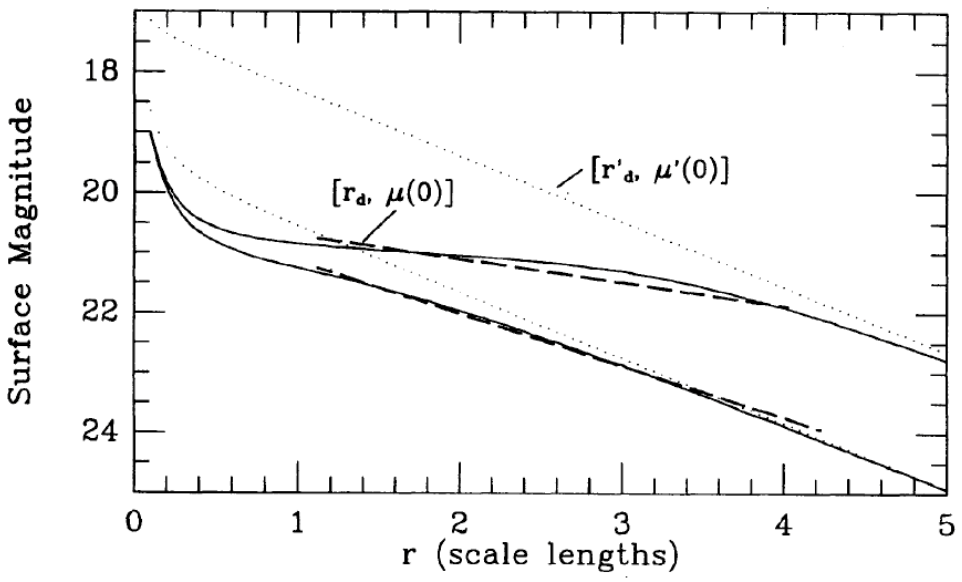

FIG. 4. Dramatization of the effects of absorption on photometric profiles. *Lower solid line*: profile of a low inclination disk, with some absorption in inner parts; *lower dotted line*: unabsorbed, exponential stellar disk with scale length r'_d plus a bulge with 7% of total light; *lower heavy-dash line*: exponential fit to absorbed profile between 1.1 and 4.2 scale lengths r'_d. *Upper solid line*: same galaxy profile seen highly inclined to the line of sight; *upper dotted line*: unabsorbed profile of the inclined disk; *upper heavy-dash line*: exponential fit to absorbed, inclined profile, between 1.1 and $4.0r'_d$, yielding fit parameters $[r_d, \mu(0)]$. Ordinate scale is arbitrary.

[Giovanelli *et al.* 1994, *A.J.*, **107, 2036**]

• The stellar density perpendicular to the disk of a galaxy can also be parameterized as an exponential. However, the vertical scale length differs for different types of stars. Below are some rough vertical scale lengths for stars in solar neighborhood:

Object	Scale Length (pc)
O stars	50
Cepheids	50
B stars	60
Open Clusters	80
Interstellar Medium	120
A stars	120
F stars	190
Planetary Nebulae	260
G Main Sequence Stars	340
K Main Sequence Stars	350
White Dwarfs	400
RR Lyr Stars	2000

• For a long time, it was thought that the central surface brightness of spiral disks was approximately $B \sim 21.65 \pm 0.3$ mag arcsec^{-2}) for all galaxies; this was known as the Freeman law. But, with the advent of CCDs, this was discovered to be a selection effect – it is easy to identify high surface brightness objects than low surface brightness objects. While the central surface brightness of spiral disks seldom get brighter than $B \sim 21.7$, the distribution of fainter central surface brightnesses is roughly flat.

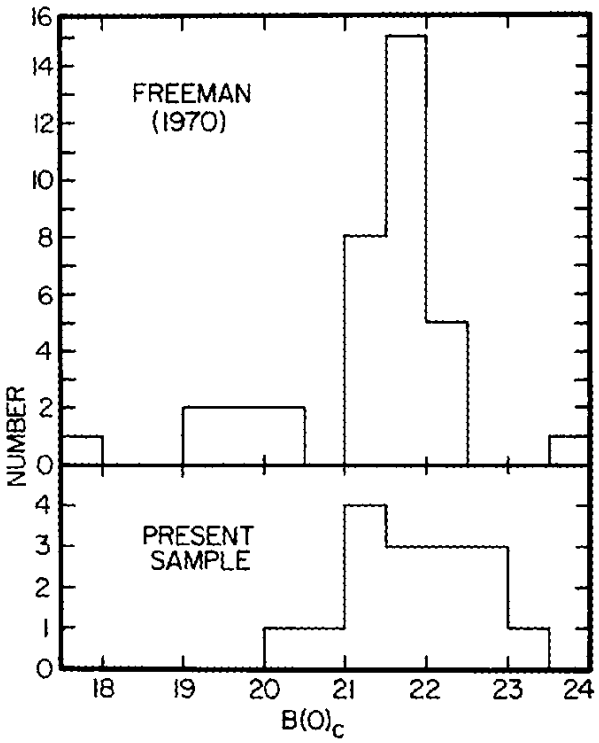

FIG. 7.—The distribution of disk central surface brightness in this study (*lower panel*) and in the study of Freeman (1970) (*upper panel*).

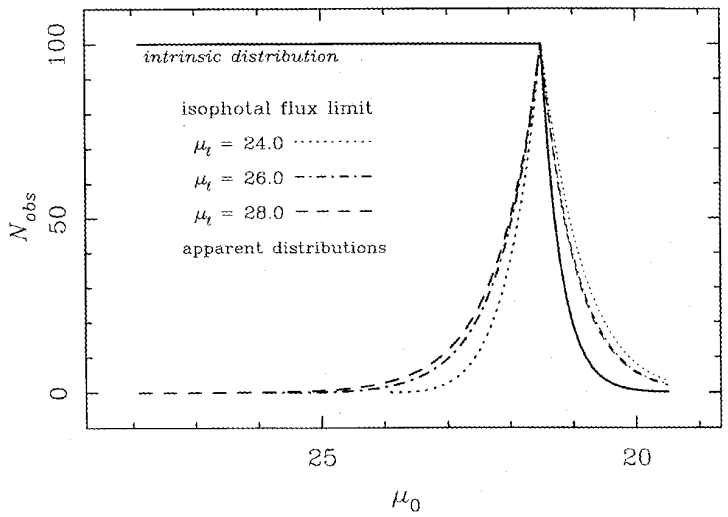

Figure 3. As in Fig. 2, but for catalogues limited by isophotal magnitude. The apparent distribution of μ_0 is even sharper than in the diameter-limited case because $N_{obs} \propto 10^{-0.6(\mu_0 - \mu_l)}$ rather than $(\mu_l - \mu_0)^3$.

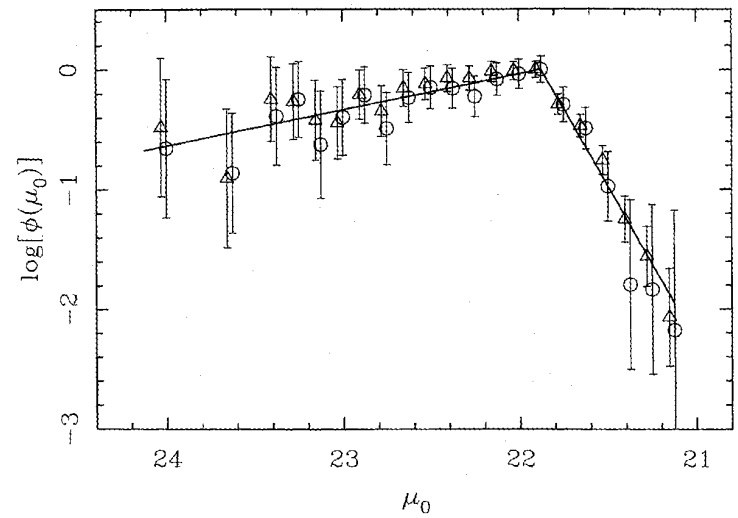

Figure 5. The surface brightness distribution derived from the data of Davies (1990). Circles are data selected by diameter, while triangles are magnitude-limited data. Error bars are from counting statistics. The line is a least-squares fit to the data giving equal weight to points from diameter- and magnitude-limited samples. The distribution declines slowly faintwards of the Freeman value, indicating a large space density of low surface brightness galaxies. It cuts off sharply brightwards of μ_0^* in analogy with the turndown of the luminosity function at L^*.

[Freeman 1970, *Ap.J.*, **160,** 811]
[Boroson 1981, *Ap.J.Supp.*, **46,** 177]
[McGaugh 1996, *MNRAS,* **280,** 337]

• Bright spirals are more metal rich than faint spirals. Similarly, early-type (Sa, Sb) spirals are, in general, more metal-rich than equivalent late-type (Sc, Sd) spirals.

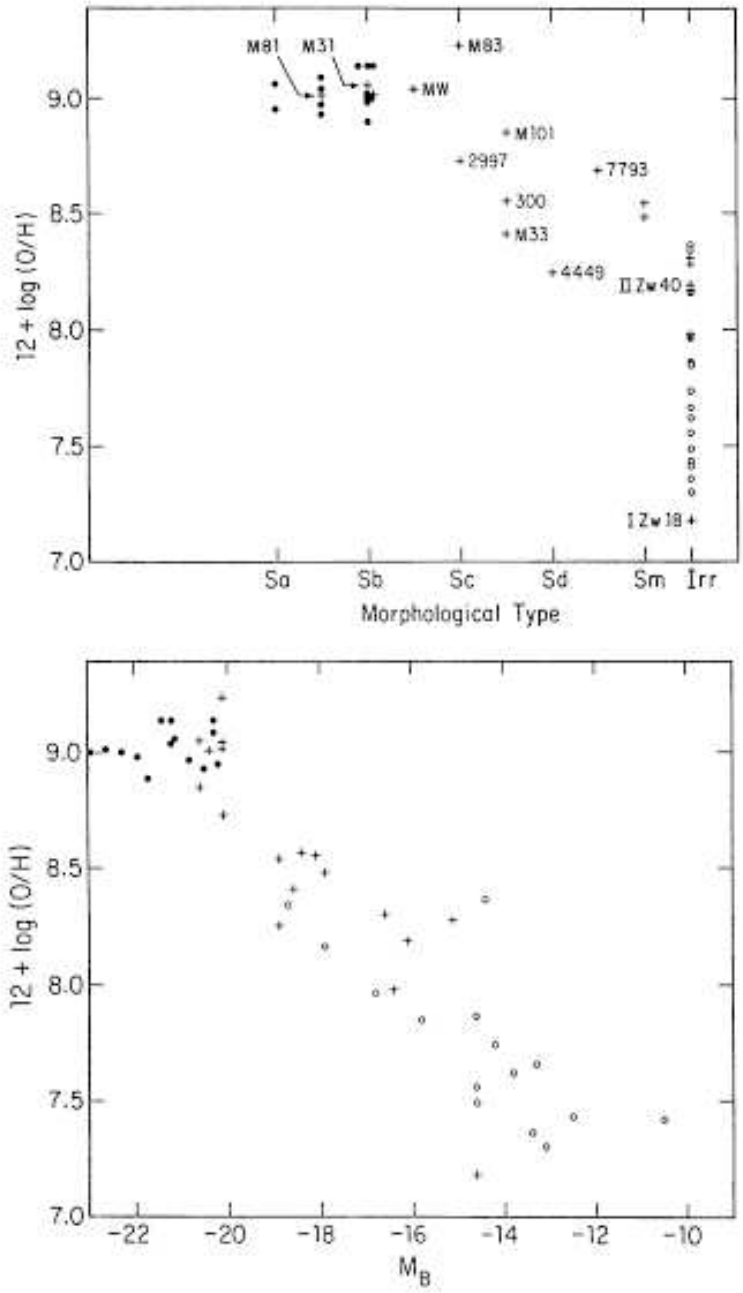

Figure 7 O/H abundance vs morphological type (*upper*) and absolute magnitude (*lower*). Different symbols represent different sources: filled circles—Oey & Kennicutt (1993), plus signs—Garnett & Shields (1987), open circles—Skillman et al (1989). The absolute magnitudes are as given in these references.

[Roberts & Haynes 1994, *A.R.A.A.*, **32,** 115]

• Most spirals have radial metallicity gradients. The gradients appear to be shallower in early-type systems, but are still present.

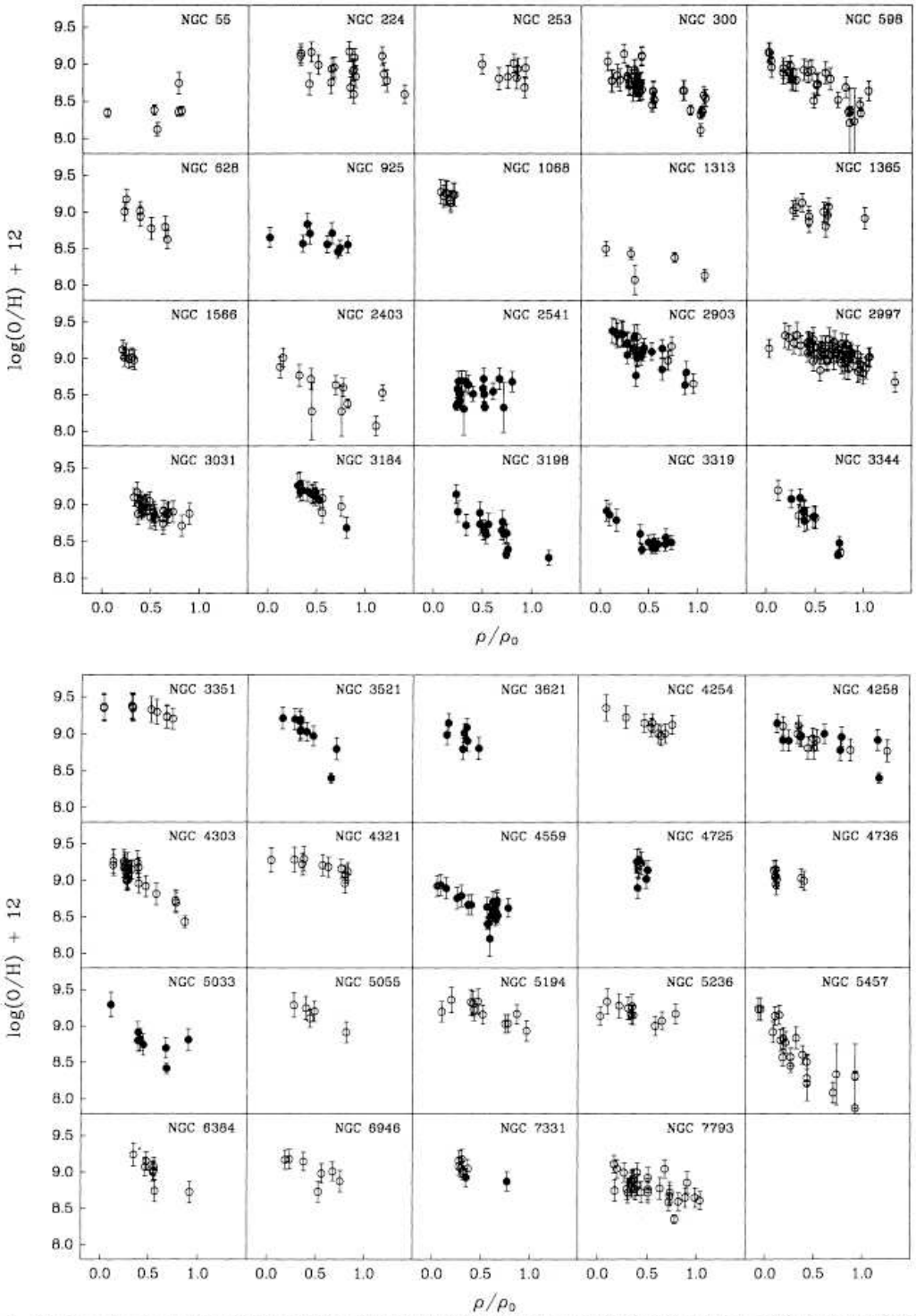

FIG. 8.—Abundances for spiral galaxies with more than five H II regions observed are plotted vs. fractional isophotal radius (= radius/isophotal radius). Our data are presented with filled circles, while that from the literature is presented with open circles.

[Zaritsky, Kennicutt, & Huchra 1994, *Ap.J.*, **420,** 87]

• Spiral galaxies typically have "flat" rotation curves, that do not decline with radius. This suggests that the dominant source of matter in the galaxy is in the form of an isothermal halo. To see this, consider that for circular orbits,

$$\frac{G\mathcal{M}(r)}{r^2} = \frac{v_c^2}{r} \tag{7.02}$$

Now at large radii, even non-singular isothermal spheres follow an $\rho \propto r^{-2}$ density law. In that case, the mass contained within within a radius R is

$$\mathcal{M}(R) = \int_0^R 4\pi r^2 \rho(r)\, dr = \int_0^R 4\pi r^2 \frac{\rho_0}{r^2} dr = 4\pi\rho_0 R \tag{7.03}$$

Thus,

$$\frac{G\left(4\pi\rho_0 R\right)}{R^2} = \frac{v_c^2}{R} \tag{7.04}$$

or

$$v_c = \left(4\pi G\rho_0\right)^{1/2} \tag{7.05}$$

In other words, a flat rotation law.

• Of course, spiral disks do contain some mass, and, in the inner parts of spirals, measured mass to light ratios are consistent with little, if any dark matter. At larger radii, the disk-mass declines and the halo mass increases just enough to keep the rotation curve flat. Thus, there appears to be a "disk-halo conspiracy."

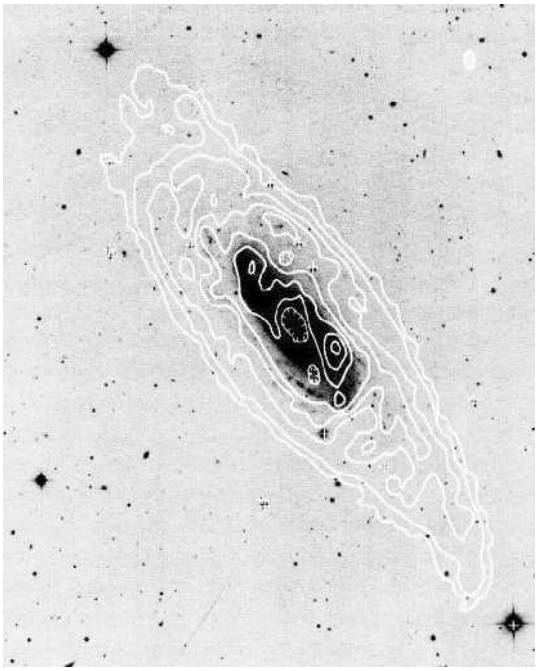

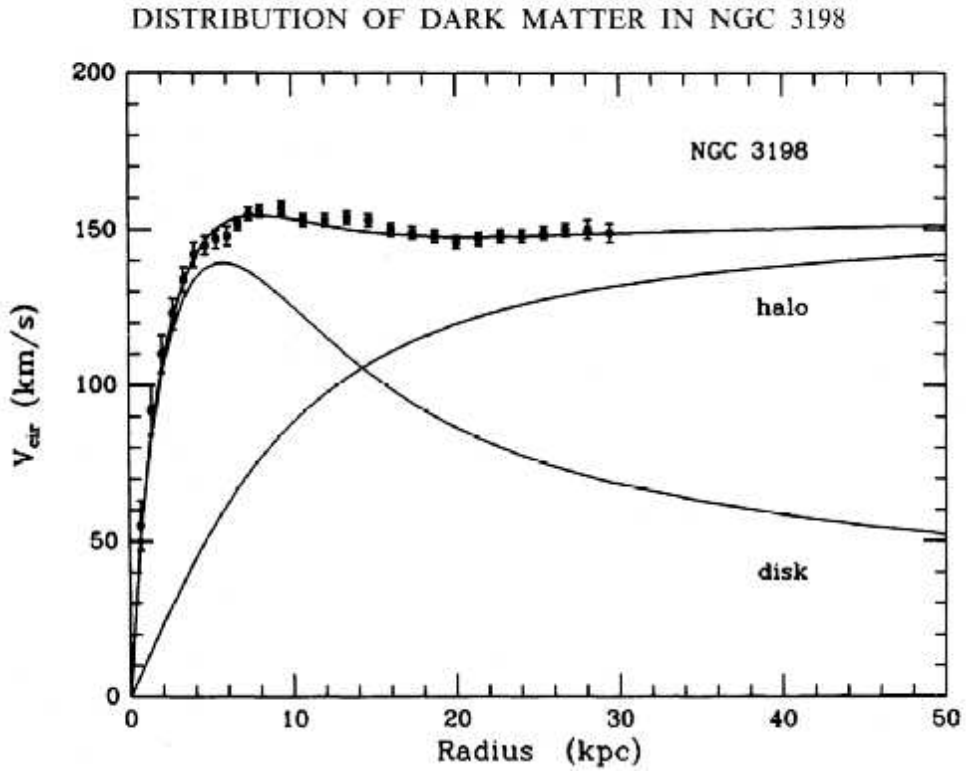

[van Albada *et al.* 1985, *Ap.J.*, **295,** 305]

• There is a tight relation ($< 20\%$) between a spiral galaxy's rotation rate and its total luminosity. For circular orbits,

$$\frac{G\mathcal{M}m}{r^2} = \frac{mv_{\rm circ}^2}{r} \quad \Longrightarrow \quad \frac{\mathcal{M}}{r^2} \propto v^2 \tag{7.06}$$

The luminosity-line width (or Tully-Fisher relation) says that

$$\mathcal{L} \propto v^a \tag{7.07}$$

where a depends on the bandpass of the observations. (For the B-band, $a \sim 2.9$, but for the infrared (where internal extinction is unimportant), the exponent is ~ 3.5. Obviously, the two equations put together imply that

$$\mathcal{L} \propto \left(\frac{\mathcal{M}}{r}\right)^{a/2} \tag{7.08}$$

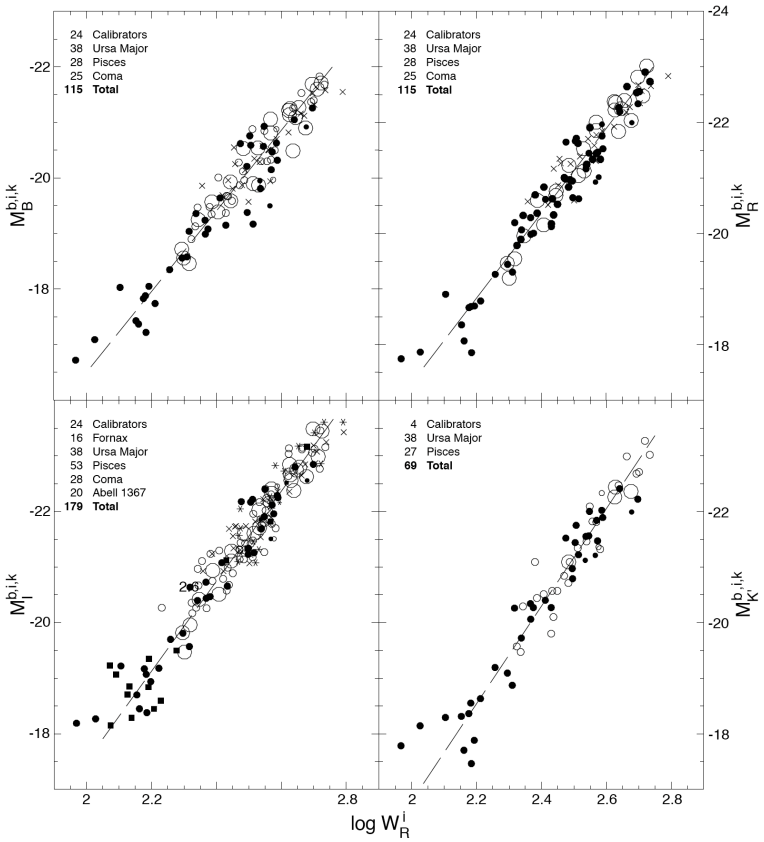

FIG. 6.—*B*, *R*, *I*, and *K′* absolute magnitude–line width relations for the cluster template galaxies translated to overlay on the zero-point calibrator galaxies. Symbols and straight line fits as in previous plots. The *I* relation involves five clusters and 24 zero-point calibrators, the *B* and *R* relations are built with three clusters and 24 zero-point calibrators, and the *K′* relation is based on two clusters and four zero-point calibrators. Relative distances between clusters and with respect to the calibrators are the same on all plots.

[Tully & Pierce 2000, *Ap. J.*, **533,** 744]

Properties of Dwarf Galaxies

[Mateo 1998, *A.R.A.A.*, **36,** 435]

Dwarf galaxies have very different properties from either spiral or elliptical galaxies. Normally, dwarf galaxies are defined as objects with absolute B magnitudes fainter than -16. There are three types of dwarf galaxies: dwarf ellipticals (dE), dwarf spheroidals (dSph), and dwarf irregulars (dI). Unfortunately, astronomers are *very* sloppy in their terminology, so it is sometimes hard to understand which type is being talked about.

Dwarf Ellipticals are the low luminosity extension of normal giant elliptical galaxies; they obey the same relation as their larger counterparts. An example of a dwarf elliptical is M32. (Actually, M32 is more compact than a normal elliptical, since it has been tidally stripped of its outer stars by M31.)

Dwarf Spheroidals are gas-poor, diffuse systems whose density profile is closer to an exponential disk than an $r^{1/4}$ law. These objects do not fall on the elliptical galaxy fundamental plane, and, in the Morgan classification scheme, would be given the letter "D " instead of "E". Examples are NGC 147 and the Leo I dwarf.

Dwarf Irregulars are low-luminosity extensions to spiral galaxies. In general, these objects are brighter than the dSph galaxies since they have active star formation, but if their star formation were to cease, they might evolve into a dSph. The Small Magellanic Cloud is a dwarf irregular.

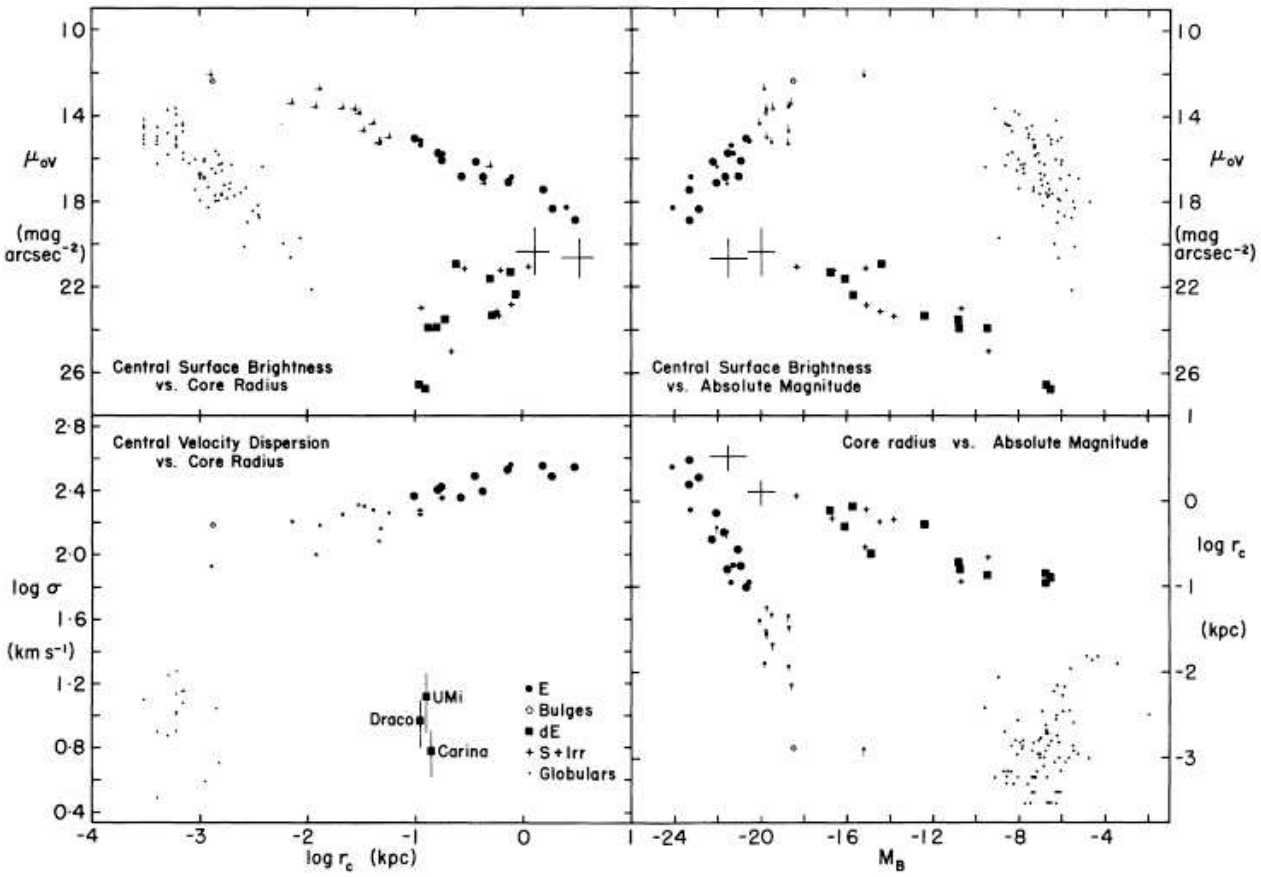

FIG. 3.—Comparison of the core parameter relations for various kinds of stellar systems. Bulges and ellipticals are as in Fig. 2. The dwarf elliptical galaxies are, in order of decreasing luminosity, IC 3349, 12h52, and 13h66 (Virgo Cluster designations from Binggeli, Sandage, and Tarenghi 1984), NGC 147, Fornax, Leo I, Sculptor, Leo II, Draco, Carina, and UMi. Similarly, the dS+Irr galaxies are the generic large disk (two points), LMC, SMC, NGC 6822, WLM, IC 1613, Sextans A, GR 8, and LGS-3. The discrepant globular cluster at upper left ($\mu_{0V} = 16.38$ mag arcsec^{-2}, log $r_c = -2.42$) is, of course, ω Cen.

[Kormendy 1985 *Ap. J.*, **295,** 73]

Dwarf galaxies have the following properties:

• Dwarf galaxies are typically very metal poor (but not as metal-poor as a Pop II globular cluster).

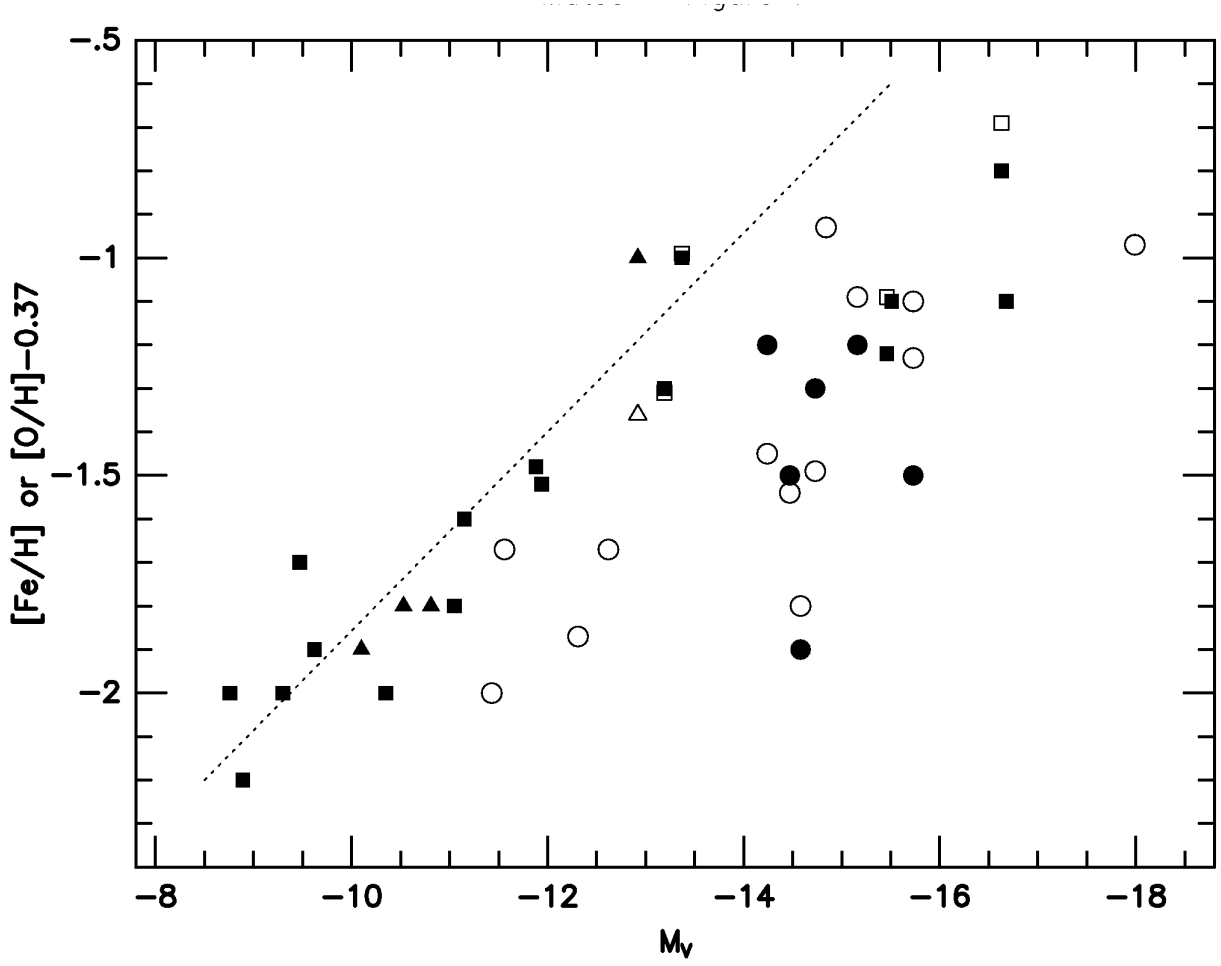

[Mateo 1998, *A.R.A.A.*, **36,** 435]

• Dwarf galaxies show evidence for more than one burst of star formation. (As we'll see, this is a very curious feature.)

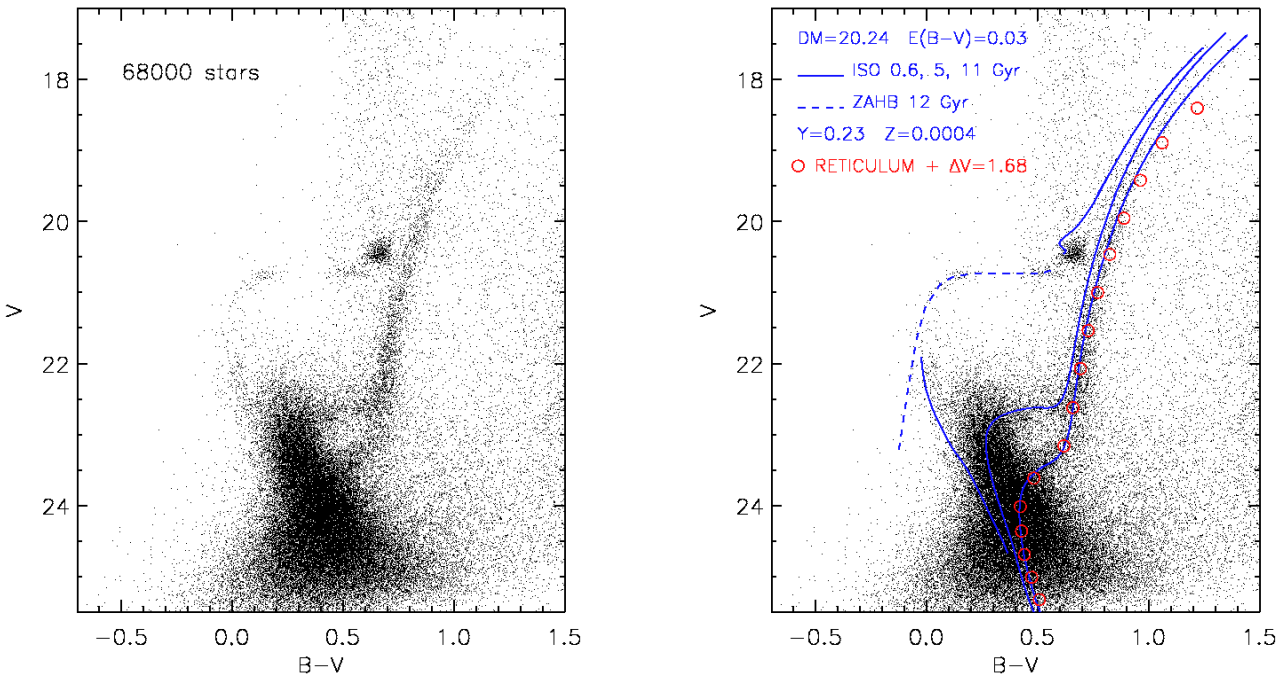

[Monelli *et al.* 2003 *A.J.*, **126,** 218]

• Dwarf galaxies can be "nucleated." Their nuclei are sometimes interpreted as being a small bulge.

• The mass-to-light ratio of dwarf spheroidals (as found from individual stellar kinematics) can be extremely large!

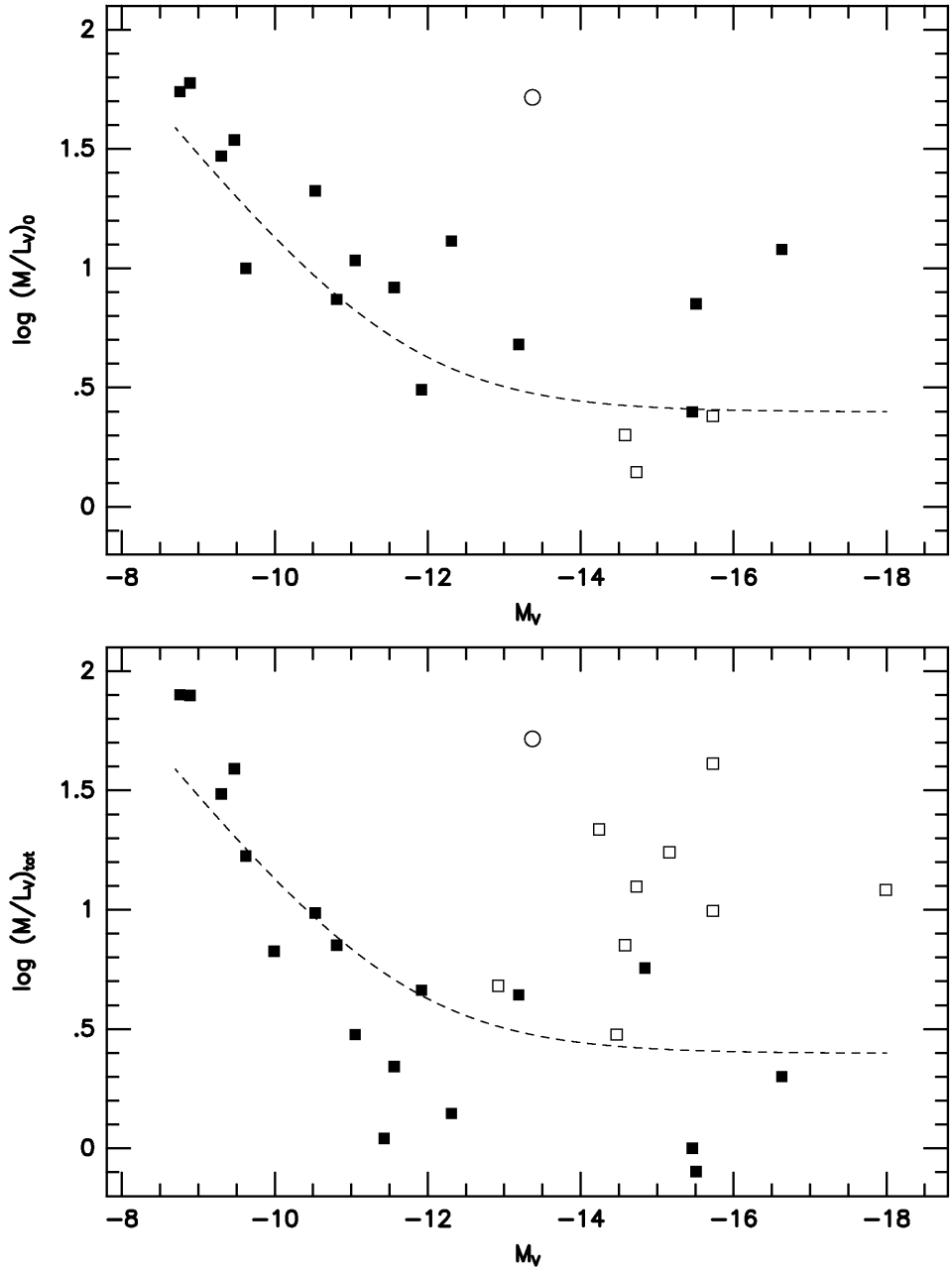

[Mateo 1998, *A.R.A.A.*, **36,** 435]